CrystEngComm

ROYAL SOCIETY OF CHEMISTRY

PAPER

View Article Online
View Journal | View Issue

Cite this: *CrystEngComm*, 2025, **27**, 1960

Extremely effective separations of pyridine/picoline mixtures through supramolecular chemistry strategies employing (4*R*,5*R*)-bis(diphenylhydroxymethyl)-2-spiro-1′-cyclohexane-1,3-dioxolane as the host compound†

Daniella L. Recchia,* Benita Barton and Eric C. Hosten

The present investigation focussed on assessing the ability of (4*R*,5*R*)-bis(diphenylhydroxymethyl)-2-spiro-1′-cyclohexane-1,3-dioxolane (TADDOL6) to separate pyridine/methylpyridine (picoline) mixtures through supramolecular chemistry protocols. At the outset, TADDOL6 was revealed to possess the ability to form 1:1 host:guest inclusion compounds with each of pyridine (PYR) and 2-, 3- and 4-methylpyridine (2MP, 3MP and 4MP) in single solvent crystallization experiments. This host compound, furthermore, demonstrated enhanced selectivities in PYR/MP mixtures: preferred guests were PYR and 3MP (in the absence of PYR), followed by 4MP and then 2MP. Subsequent binary guest competition experiments showed that TADDOL6 may be employed in order to effectively separate very many of these mixtures in this way, and significant selectivity coefficients (*K*) were calculated in numerous instances. Single crystal X-ray diffraction (SCXRD) experiments showed that the only significant (host)π···π(guest) stacking interactions were those between TADDOL6 and the preferred PYR and 3MP guest molecules, while a consideration of Hirshfeld surfaces demonstrated that these preferred guests were involved in a tighter packing motif with TADDOL6 than those with 2MP and 4MP. Results from thermal analyses, more specifically when determining the guest release onset temperatures (T_{on}) and the enthalpies associated with these release processes, also agreed with the host selectivity order in the mixed guest competition experiments.

Received 28th January 2025,
Accepted 25th February 2025

DOI: 10.1039/d5ce00111k

rsc.li/crystengcomm

1. Introduction

The separation of the methylpyridines (2MP, 3MP and 4MP), also known as the picolines, remains a considerable challenge in the chemical industry.[1–6] Current methods involve, as salient examples, azeotropic fractional distillations, zeolites and macrocyclic crystalline cucurbiturils. Many of these separatory methods are costly in both economic and energy terms, and oftentimes furnish these solvents with purities that are not acceptable for subsequent applications. These separations are problematic as a result of the very similar physical properties of these solvents: 2MP, 3MP and 4MP boil between 128 and 145 °C. More especially, 3MP (b.p. 144 °C) and 4MP (b.p. 145 °C) cannot be effectively separated by fractional distillations without extensive energy resources.

It is important that 2MP, 3MP and 4MP are isolated in pure form as each one has unique roles in the chemical industry.[7,8] For example, 2MP is used to produce the monomer 2-vinylpyridine which is used in the production of resins, 3MP is a reagent in the production of the downstream pesticide chlorpyrifos, and 4MP is a starting material for the anti-tuberculosis drug, isoniazid.

The first known synthesis towards PYR was reported by Chichibabin *et al.* in 1924.[9] This condensation reaction employed formaldehyde, ammonia and acetaldehyde as starting materials in the presence of aluminium oxide. Subsequent to that work, many other methods have been reported in the literature for the preparation of PYR and the MPs, more usually using the same reactants but altering the

Department of Chemistry, Nelson Mandela University, PO Box 77000, Port Elizabeth, 6031, South Africa. E-mail: s220241104@mandela.ac.za

† Electronic supplementary information (ESI) available: The crystal structures of complexes TADDOL6·PYR, TADDOL6·2MP, TADDOL6·3MP and TADDOL6·4MP were deposited at the Cambridge Crystallographic Data Centre (CCDC) and their CCDC numbers are 2341183–2341186. The ^{1}H-NMR spectra for all of the mixed complexes prepared from the equimolar guest experiments were also deposited in the ESI, together with the ORTEP diagrams for the four complexes and tables summarising the various parameters of the short contacts observed in the four complexes. For ESI and crystallographic data in CIF or other electronic format see DOI: **https://doi.org/10.1039/d5ce00111k**

nature of the catalyst to include various SiO_2–Al_2O_3 combinations,[10–12] and ZSM-5 (ref. 13–15) and HZSM-5 (ref. 16–18) zeolitic catalysts with or without added metals. Unfortunately, many synthetic strategies furnish mixtures of PYR/MPs and hence is required subsequent and difficult separations of these isolated mixtures.[19,20]

Owing to the extremely challenging and often ineffective separation strategies that currently exist for these pyridyl mixtures, alternative, more effective and less costly approaches remain appealing. The field of supramolecular chemistry[21,22] may serve as just such an alternate method. This field of science relies on the presence of weak and reversible noncovalent bonds (hydrogen bonding, π···π stacking, C–H···π close contacts, *etc.*) between two different species, that is, the host and the guest compound, in order to form an inclusion compound. These complexes may be prepared by means of a simple crystallization procedure of the host from the guest solvent. Effective separations are possible if the host compound possesses an affinity for one guest species only when crystallized from a mixture of guests. There exist many reports in the literature where this field of chemistry has been investigated for the separation of these pyridines.[23,24] In our own laboratories, host compounds based on tartaric acid,[25] xanthenyl, thioxanthenyl and other tricyclic fused systems,[26,27] anthracene,[28] as well as molecules bearing the wheel-and-axle design,[29] have all been explored for their separation potential for these mixtures in search of better effectivity and, also, complementary host selectivity behaviours. These reports all allude to the feasibility of using supramolecular chemistry for the required separations, and overwhelming host affinities were, oftentimes, observed in crystallization experiments from these mixed guests; the preferred guest of the host species was dependent upon the structure of the host compound, with each of PYR and the MPs having a host compound with a preference for it. As such, a chemist is able to select an appropriate host compound to sequester the required guest species of interest from the mixture.

In the present work, host compound (4*R*,5*R*)-bis(diphenylhydroxymethyl)-2-spiro-1′-cyclohexane-1,3-dioxolane (TADDOL6), also derived from inexpensive and naturally occurring tartaric acid, was presented with various mixtures of PYR/MPs in order to assess its ability for their separation (Scheme 1). Single solvent inclusion complexes were subjected to both SCXRD and thermal analyses to elucidate the mode of enclathration and to explain any host preferential behaviour observed in the mixed guest competition experiments. To date, TADDOL6 has not been employed in this manner, and the results presented here are entirely novel. Herein we report on all the findings that were thus obtained.

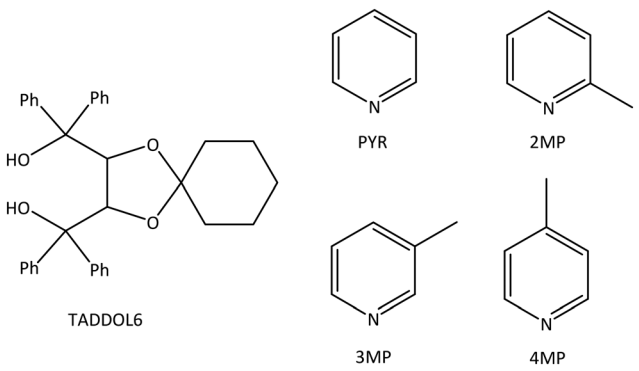

Scheme 1 Molecular structures of TADDOL6 and PYR and the three MP isomers.

2. Experimental

2.1 General

The guest solvents and the starting materials for the synthesis of TADDOL6 were purchased from Merck (South Africa) and used without further modification.

^{1}H-NMR experiments were carried out in $CDCl_3$ (as the deuterated solvent). The applicable instrument was a Bruker Ultrashield Plus 400 MHz NMR spectrometer, and the obtained data were analysed by means of Topspin 4.3.0 software.

The complexes TADDOL6·PYR, TADDOL6·2MP, TADDOL6·3MP and TADDOL6·4MP were analysed by means of SCXRD experiments. Two instruments were employed. The first was a Bruker Kappa Apex II diffractometer with graphite-monochromated MoKα radiation (λ = 0.71073 Å). The resulting X-ray data were collected and analyzed by means of APEXII[30] data software. Cell refinement and data reduction were performed using the SAINT program. All numerical absorption corrections were carried out using SADABS. The structure of each crystal was solved with SHELXT-2018/2[31] and refined using the least-squares procedure in SHELXL-2018/3;[32] SHELXLE[33] was used as the graphical interface. All atoms, excluding hydrogen, were refined anisotropically, while all carbon- and oxygen-bound hydrogen atoms were inserted in idealized geometrical positions in a riding model. Nitrogen-bound hydrogen atoms were found on the difference Fourier map and were allowed to refine freely. The second instrument was a Bruker D8 Quest diffractometer with a Photon II CPAD detector and IμS 3.0 Mo source (Kα, λ = 0.71073 Å). Data collection was performed using APEX4,[34] and cell refinement and data reduction were carried out by means of SAINT. The numerical method implemented in SADABS[34] was used to correct the data for absorption effects. The structures of the crystals were solved using the dual-space algorithm of SHELXT-2018/2,[31] and refined using the least-squares procedures in SHELXL-2019/3. SHELXLE[33] was used as a graphical interface. Diagrams were prepared using ORTEP-3 for Windows version 2023.1.[35] All atoms, except hydrogen, were refined anisotropically, while carbon-bound hydrogen atoms were placed in calculated positions (C–H bond lengths of 0.95 Å for aromatic carbon atoms, 1.00 Å for methine and 0.99 Å for methylene) and were included in the refinement in the riding model approximation, with U_{iso}(H) set to 1.2U_{eq}(C). The hydrogen atoms belonging to

methyl groups were allowed to rotate with a fixed angle around the C–C bond to best fit the experimental electron density (HFIX 137 in the SHELXL[36] program) with U_{iso}(H) set to 1.5U_{eq}(C) and C–H bond lengths of 0.98 Å. The hydrogen atoms belonging to hydroxyl groups were allowed to rotate with a fixed angle around the C–O bond to best fit the experimental electron density (HFIX 147 in the SHELXL[36] program) with U_{iso}(H) set to 1.5U_{eq}(O) and O–H bond lengths of 0.84 Å. Wherever possible, the nitrogen-bound hydrogen atoms were located on a difference Fourier map and allowed to refine freely. If not, they were placed in calculated positions and refined by means of a riding model with U_{iso}(H) set to 1.2U_{eq}(N) and N–H bond lengths of 0.88 Å. The crystal structures of these complexes (TADDOL6·PYR, TADDOL6·2MP, TADDOL6·3MP and TADDOL6·4MP) were deposited at the Cambridge Crystallographic Data Centre (CCDC) and their CCDC numbers are 2341183, 2341184, 2341185 and 2341186, respectively.

Two gas chromatograph (GC) instruments were used in order to quantify the pyridyl guest compounds in any mixed complexes produced in this work. The first was a Young Lin YL6500 GC coupled to a flame ionization detector (GC-FID) and the second an Agilent 7890A GC coupled to an Agilent 5975C VL mass spectrometer (GC-MS). Both instruments were equipped with the same column, an Agilent J&W Cyclosil-B column (30 m × 250 μm × 0.25 μm, calibrated). The first method involved an initial 5 min hold time at 50 °C, followed by a heating ramp of 10 °C min^{-1} until 100 °C was reached. The total run time was 10 min and the flow rate 75 mL min^{-1}, while the split ratio was 1 : 50. The second method also involved an initial 5 min hold time at 50 °C, followed by a heating ramp of 5 °C min^{-1} until 100 °C was reached; the total run time was 16 min and the flow rate 120 mL min^{-1}; the split ratio was 1 : 80.

To confirm the host : guest (H : G) ratios of the single solvent complexes as obtained from the ^{1}H-NMR experiments as well as to determine their relative thermal stabilities by comparing the onset temperatures for the guest release process (T_{on}), thermal experiments were performed. The applicable instrument was a TA SDT Q600 Module system. The data were analysed using TA Universal Analysis 2000 software. The solids were isolated from their solutions by vacuum filtration and washed with low boiling petroleum ether (b.p. 40–60 °C), and then blotted dry in folded filter paper to further remove any surface solvent. Subsequently, the crystals were placed in a tared ceramic pan prior to analysis. The purge gas was high purity nitrogen, and samples were heated from approximately room temperature to 400 °C at a heating rate of 10 °C min^{-1}.

2.2 Synthesis of (4*R*,5*R*)-bis(diphenylhydroxymethyl)-2-spiro-1′-cyclohexane-1,3-dioxolane (TADDOL6)

The host compound, (4*R*,5*R*)-bis(diphenylhydroxymethyl)-2-spiro-1′-cyclohexane-1,3-dioxolane (TADDOL6), was synthesised by considering a previous report.[37] Scheme 2 illustrates the synthetic pathway towards this host species. Cyclohexanone was

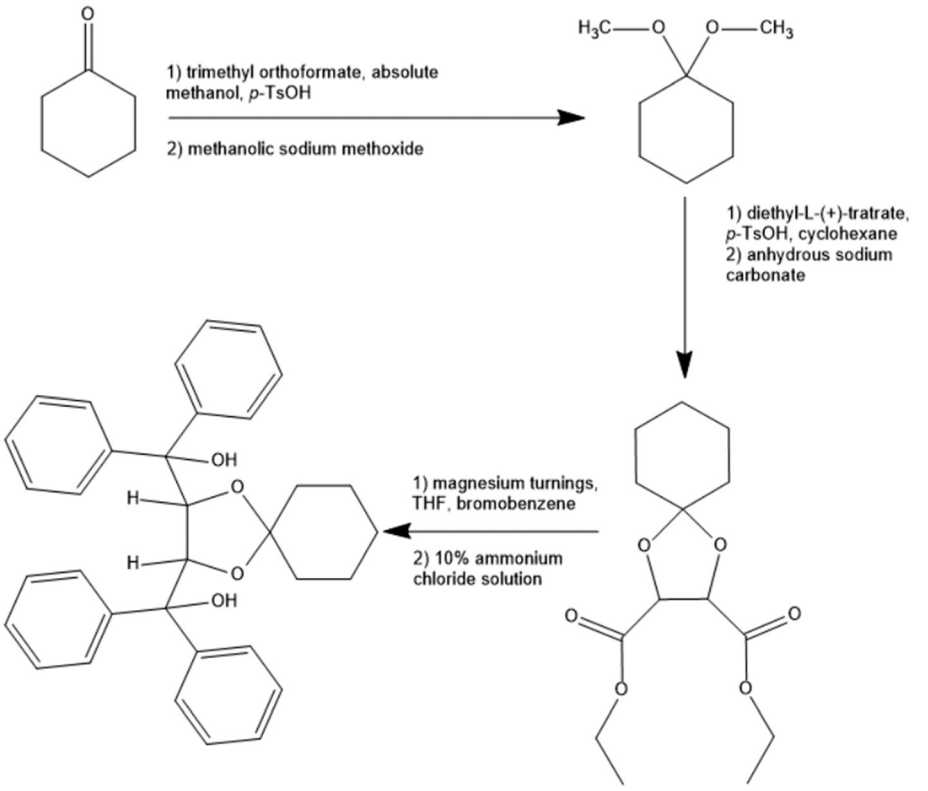

Scheme 2 Synthetic pathway towards TADDOL6.

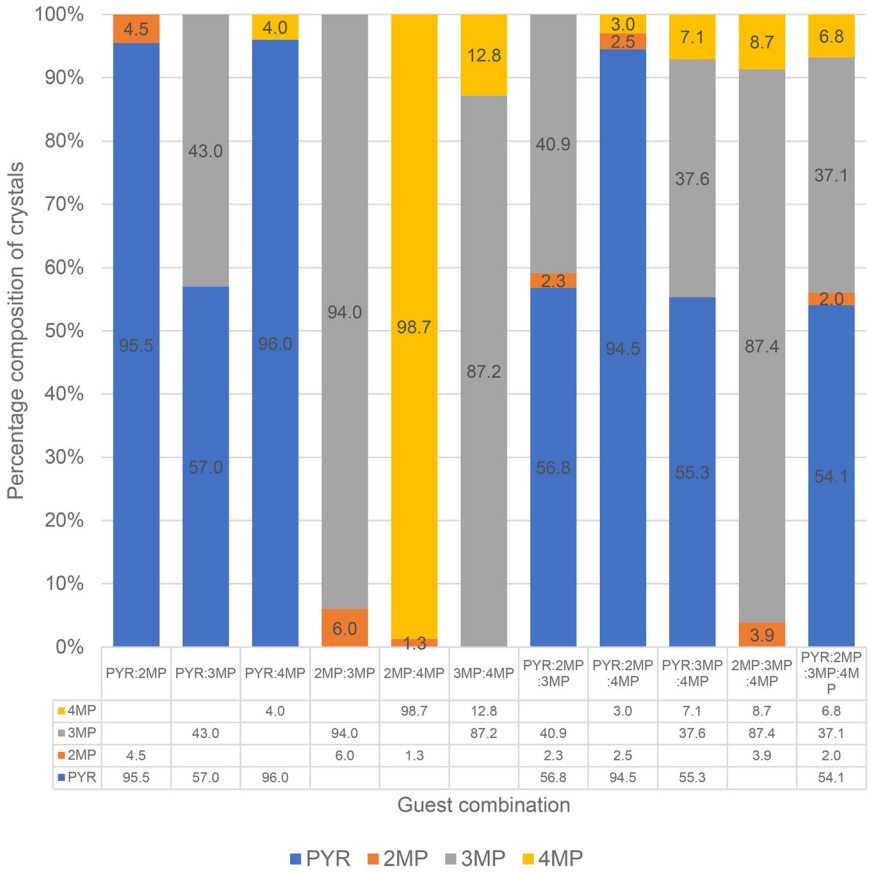

Fig. 1 Representation of the guest ratios in the equimolar mixed guest experiments with TADDOL6.

first converted to its dimethyl acetal after which this intermediate was reacted with diethyl tartrate to afford the diester. A simple Grignard addition reaction employing PhMgBr then furnished TADDOL6.

2.3 Single solvent host crystallization experiments

Approximately 0.05 g of TADDOL6 (0.09 mmol) was dissolved separately in each guest solvent in glass vials. Mild heat was applied where necessary to aid complete host dissolution. The vials were left open at ambient conditions to allow some of the solvent to evaporate off and thus to facilitate crystal growth. The formed crystals were then isolated using vacuum filtration and washed with low boiling petroleum ether (b.p. 40–60 °C) to remove any remaining guest solvent still adhering to the crystal surfaces. The washed crystals were dissolved in $CDCl_3$ and analyzed by means of ^{1}H-NMR spectroscopy, which revealed whether complexation had been successful. The H : G ratios of such formed inclusion compounds were determined through integration of applicable host and guest resonance signals on the ^{1}H-NMR spectrum.

2.4 Equimolar guest competition experiments

Guest competition experiments were conducted in glass vials by dissolving 0.05 g of TADDOL6 (0.09 mmol) in all

Table 1 Guest ratios of mixed complexes from the crystallization experiments of TADDOL6 from equimolar mixed pyridyl guests

PYR	2MP	3MP	4MP	Guest ratios/% (% e.s.d.s.)	Overall H : G ratio (unrounded)
X	X			**95.5** : 4.5 (0.4)	1 : 1 (1 : 0.9)
X		X		**57.0** : 43.0 (1.5)	1 : 1 (1 : 0.9)
X			X	**96.0** : 4.0 (0.6)	1 : 1 (1 : 0.9)
	X	**X**		6.0 : **94.0** (0.2)	1 : 1 (1 : 1.1)
	X		**X**	1.3 : **98.7** (1.3)	1 : 1 (1 : 1.2)
		X	X	**87.2** : 12.8 (4.7)	1 : 1 (1 : 1.0)
X	X	X		**56.8** : 2.3 : 40.9 (4.5) (0.03) (4.5)	1 : 1 (1 : 1.1)
X	X		X	**94.5** : 2.5 : 3.0 (0.5) (0.2) (0.7)	1 : 1 (1 : 0.9)
X		X	X	**55.3** : 37.6 : 7.1 (2.04) (0.2) (1.9)	1 : 1 (1 : 1.1)
	X	**X**	X	3.9 : **87.4** : 8.7 (0.5) (1.8) (1.4)	1 : 1 (1 : 1.0)
X	X	X	X	**54.1** : 2.0 : 37.1 : 6.8 (3.1) (0.1) (2.1) (0.3)	1 : 1 (1 : 1.2)

possible equimolar combinations of guest mixtures (5 mmol combined amount). The vials were then closed and stored at approximately 4 °C to allow crystal formation. The formed crystals were isolated and processed as described in the single solvent host crystallization experiments. The guest ratios in any mixed complexes formed in this way were determined by means of GC analyses, while the overall H : G ratios were obtained using ^{1}H-NMR spectroscopy.

2.5 Binary guest competition experiments where the molar ratios of the two guests present were systematically varied

These experiments were carried out in glass vials by dissolving 0.05 g of TADDOL6 (0.09 mmol) in binary guest mixtures (5 mmol combined amount), where the amount of each guest was varied to include the molar ratios 20 : 80, 40 : 60, 60 : 40 and 80 : 20 (guest A (G_A) : guest B (G_B)). The vials were closed and stored at approximately 4 °C, and crystallization thus proceeded. The crystals were isolated and treated as before. The guest ratios in the mixed complexes were determined through GC analyses. Selectivity profiles were then constructed by plotting the amount of G_A (or G_B) in the crystals (Y) against the concentration of the same guest in the original solution (X). The selectivity coefficient, K, which serves as a measure of the host selectivity in these conditions, was calculated by means of the equation of Pivovar and co-workers, $K_{G_A:G_B} = Y_{G_A}/Y_{G_B} \times X_{G_B}/X_{G_A}(X_{G_A} + X_{G_B} = 1)$.[38] $K = 1$ signifies an unselective host compound and this is

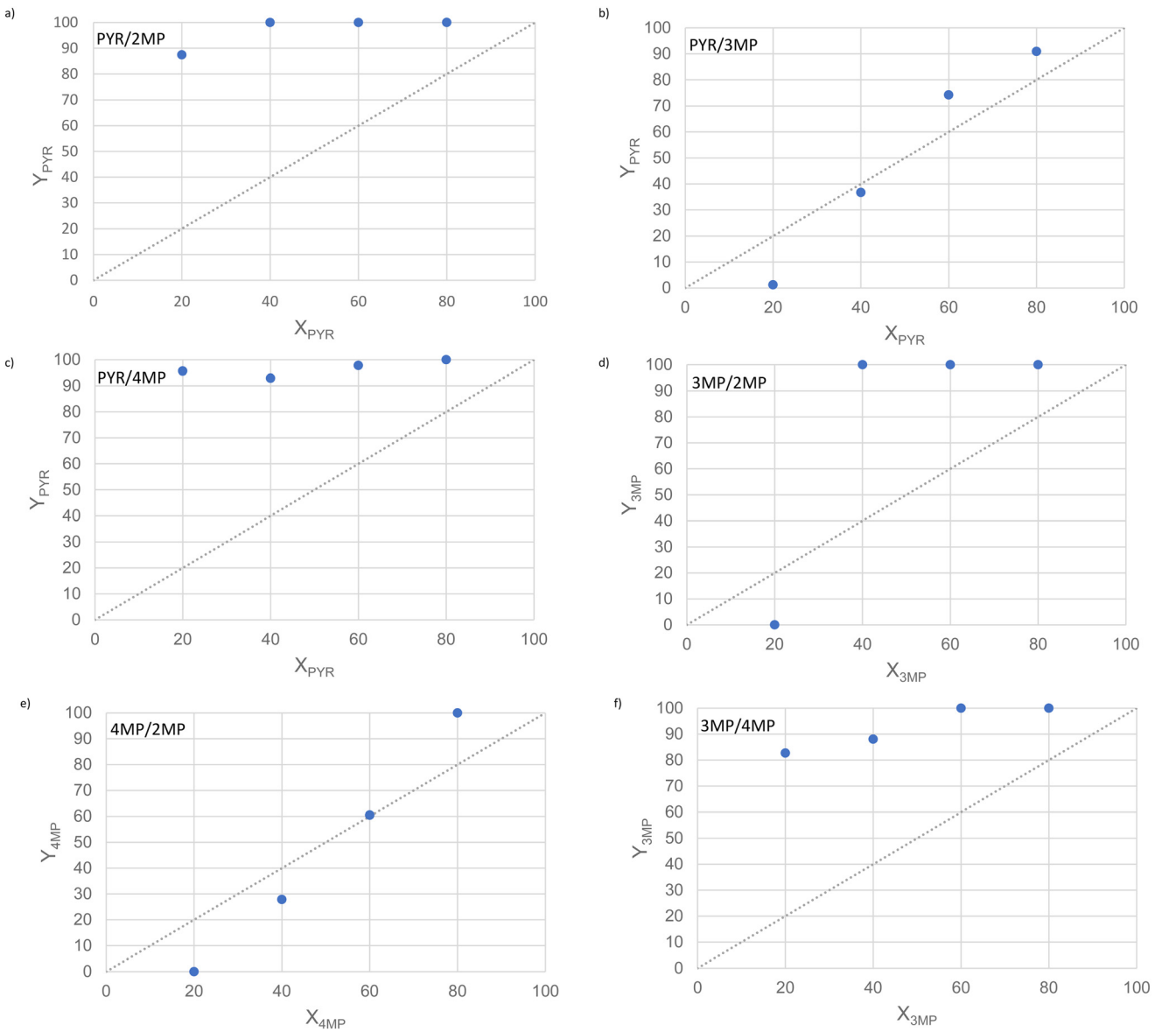

Fig. 2 Selectivity profiles for TADDOL6 in (a) PYR/2MP, (b) PYR/3MP, (c) PYR/4MP, (d) 3MP/2MP, (e) 4MP/2MP and (f) 3MP/4MP binary mixtures, where the straight diagonal lines represent a host compound that is not selective.

Table 2 Relevant crystallographic data for the pyridyl complexes of TADDOL6

	TADDOL6·PYR	TADDOL6·2MP	TADDOL6·3MP	TADDOL6·4MP
Chemical formula	$C_{34}H_{34}O_4{\cdot}C_5H_5N$	$C_{34}H_{34}O_4{\cdot}C_6H_7N$	$C_{34}H_{34}O_4{\cdot}C_6H_7N$	$C_{34}H_{34}O_4{\cdot}C_6H_7N$
Formula weight [g mol^{-1}]	585.71	599.74	599.74	599.74
Crystal system	Orthorhombic	Monoclinic	Triclinic	Triclinic
Space group	$P2_12_12_1$	$P2_1$	$P1$	$P1$
a [Å]	9.6215(4)	9.3884(4)	9.5704(6)	9.3267(9)
b [Å]	10.7098(4)	34.6497(13)	9.8658(5)	9.9858(10)
c [Å]	29.8886(12)	10.1379(4)	17.3649(10)	18.1928(19)
Alpha [°]	90	90	97.408(2)	81.945(4)
Beta [°]	90	92.6305(17)	100.565(2)	78.493(4)
Gamma [°]	90	90	90.588(2)	87.890(4)
V [Å^3]	3079.9(2)	3294.4(2)	1597.37(16)	1643.9(3)
Z	4	4	2	2
D(calc) [g cm^{-3}]	1.263	1.209	1.247	1.212
μ(Mo-Kα) [mm^{-1}]	0.081	0.077	0.080	0.077
F(000)	1248	1280	640	640
Temperature [K]	200	200	200	200
$\Theta_{min-max}$ [°]	2.2, 28.3	2.0, 26.4	2.1, 28.3	2.1, 28.3
Total data	69 975	84 228	135 115	159 107
Unique data	7631	13 432	15 818	16 225
R_{int}	0.067	0.029	0.038	0.058
Observed data [$I > 2.0\sigma(I)$]	6756	13 132	14 346	14 347
Restraints	0	265	3	3
N_{ref}	7631	13 432	15 818	16 225
N_{par}	400	845	818	818
R	0.0460	0.0423	0.0381	0.0466
wR_2	0.0907	0.1135	0.0794	0.1032
S	1.12	1.07	1.06	1.13
Min. resd. dens. [e Å^{-3}]	−0.24	−0.25	−0.19	−0.32
Max. resd. dens. [e Å^{-3}]	0.25	0.33	0.24	0.39

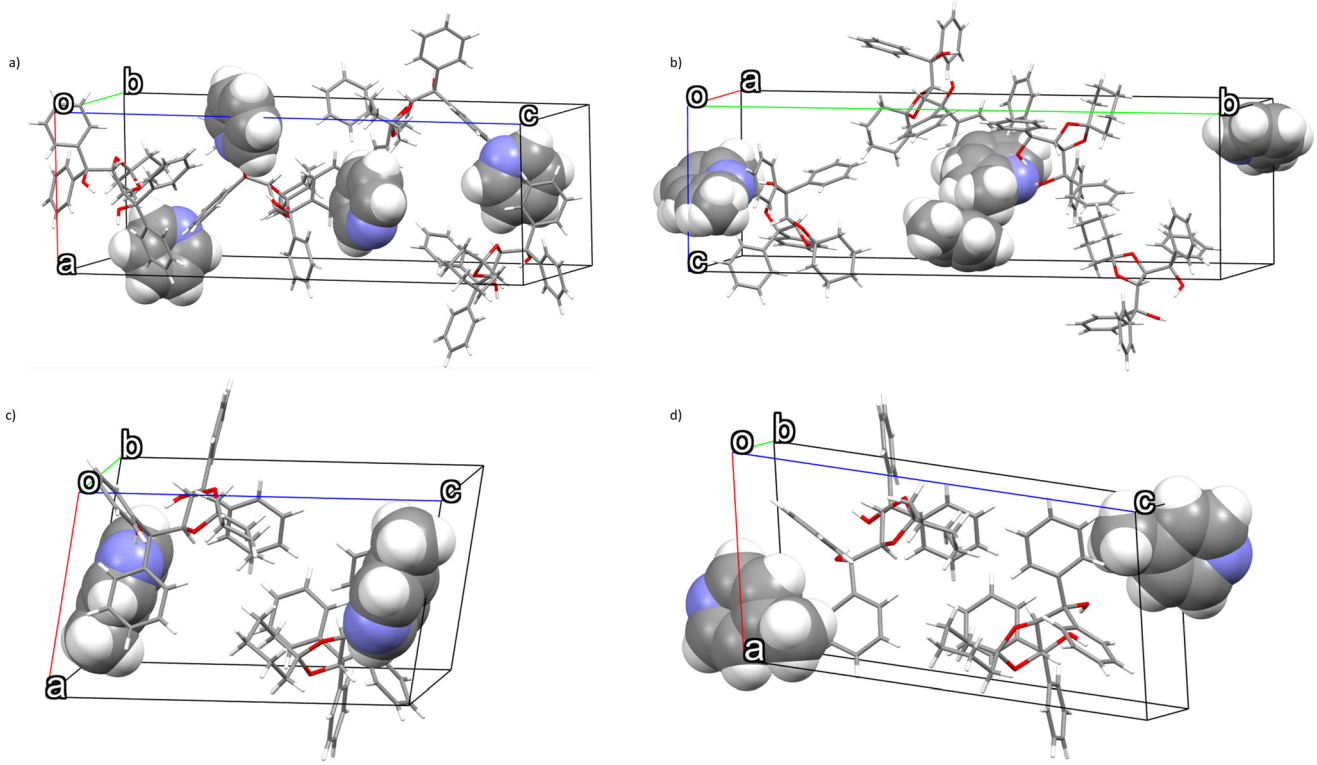

Fig. 3 The unit cells of (a) TADDOL6·PYR, (b) TADDOL6·2MP, (c) TADDOL6·3MP and (d) TADDOL6·4MP. The host molecules are in capped-stick and the guest structures in spacefill representation.

represented by the diagonal straight line that has been inserted into each selectivity profile for facile comparison with the experimentally obtained data points.

2.6 Software

The program employed to prepare all the crystal structure diagrams, including void figures, was Mercury.[39] In order to obtain the latter figures, the spaces that formed upon deleting each of the guest molecules from the packing calculations were investigated by means of a probe with a radius of 1.2 Å. All bond angles and lengths, covalent and noncovalent, were also obtained by means of this program. Additionally, program Crystal Explorer version 21.5 was required in order to quantify the guest···host interactions in each of the complexes. At the outset were prepared three-

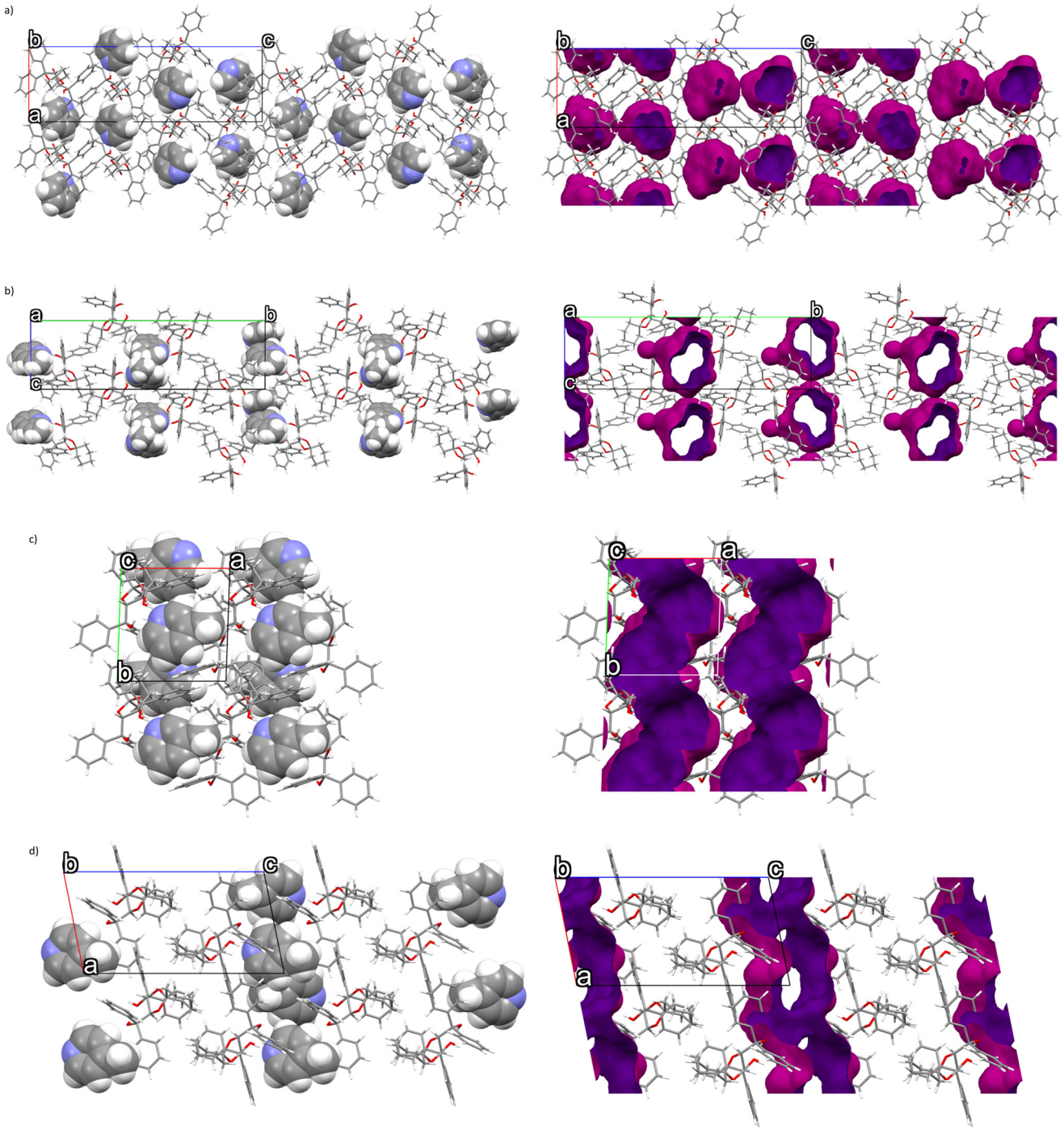

Fig. 4 Host–guest packing (left) and voids (right) in (a) TADDOL6·PYR, (b) TADDOL6·2MP, (c) TADDOL6·3MP and (d) TADDOL6·4MP. Host molecules are in capped stick form and guests in spacefill representation.

dimensional (3D) Hirshfeld surfaces around the guest molecules and, subsequently, the two-dimensional (2D) fingerprint plots were generated from these.[40,41]

3. Results and discussion

3.1 Single solvent host crystallization experiments

The resultant crystals from the single solvent host crystallization experiments were analysed using ^{1}H-NMR spectroscopy. It was observed that all four guest species were enclathrated by TADDOL6, and consistently with 1 : 1 H : G ratios.

3.2 Equimolar guest competition experiments

TADDOL6 was crystallized from each possible combination of equimolar mixed pyridyl guests, and Table 1 contains the results obtained from GC analyses. The preferred guests and their percentages are provided in bold text, and the percentage estimated standard deviations (% e.s.d.s.), owing to the experiments being carried out more than once, are also shown here.

The results obtained when PYR competed with either 2MP, 3MP or 4MP indicated that PYR was consistently the favoured guest species (the crystals contained 95.5, 57.0 and 96.0% PYR, respectively) (Table 1), with the first and last of these three results being remarkable, with near-complete selectivities towards PYR. Furthermore, the 2MP/3MP and 2MP/4MP solutions furnished complexes with significant amounts of 3MP and 4MP (94.0 and 98.7%, respectively), while the experiment involving 3MP and 4MP resulted in a complex with as much as 87.2% 3MP.

The ternary experiments involving PYR, that is, PYR/2MP/3MP, PYR/2MP/4MP and PYR/3MP/4MP, all resulted in mixed complexes enriched with PYR (56.8, 94.5 and 56.2%), while the experiment in the three isomeric methylpyridines furnished a complex that possessed significantly more 3MP (87.4%). Once more, this is an important result given the difficulty of separating 2MP/3MP/4MP mixtures by means of fractional distillations.

The quaternary equimolar guest experiment, finally, provided an overall host selectivity that was in the order PYR (54.1%) > 3MP (37.1%) > 4MP (6.8%) > 2MP (2.0%), which agreed with observations made in each of the other equimolar experiments.

Importantly, the results obtained for TADDOL6 complement those of a related host compound, (4*R*,5*R*)-bis(diphenylhydroxymethyl)-2-spiro-1′-cyclopentane-1,3-dioxolane:[42] the latter host species always preferred 3MP followed by PYR, while this order was reversed for TADDOL6 (PYR and then 3MP was favoured); however, both host compounds disfavoured 2MP and 4MP.

The overall H : G ratios were all 1 : 1, which aligns with the results of the single guest solvent experiments.

The results from Table 1 are represented graphically in Fig. 1 for facile comparison purposes.

From Fig. 1, it is clear that TADDOL6 favoured PYR and then 3MP above 2MP and 4MP in all combinations, and this confirms the selectivity of TADDOL6 to be in the order PYR > 3MP > 4MP > 2MP.

3.3 Binary guest competition experiments where the molar ratios of the two guests present were systematically varied

TADDOL6 was crystallised from binary guest mixtures, the molar ratios of which were varied in sequence, as described in the experimental section. The selectivity profiles thus obtained are provided in Fig. 2a–f.

Fig. 2a (PYR/2MP) demonstrates that TADDOL6 remained overwhelmingly selective for PYR across the concentration range when competing with 2MP. In fact, selectivities were remarkable in all of these experiments, and a solution with 20% PYR furnished crystals with as much as 87.4% of this guest species; *K* was significant here, 27.9. Moreover, the remaining three experiments (40, 60 and 80% PYR) afforded single solvent complexes only (PYR, 100.0%), and *K* was infinite in these cases. These results suggest that TADDOL6 may be employed to effectively separate all of the PYR/2MP mixtures investigated here.

The plot contained in Fig. 2b (PYR/3MP) has a characteristic S-shape indicative of the selectivity behaviour of TADDOL6 being dependent upon the concentrations of the

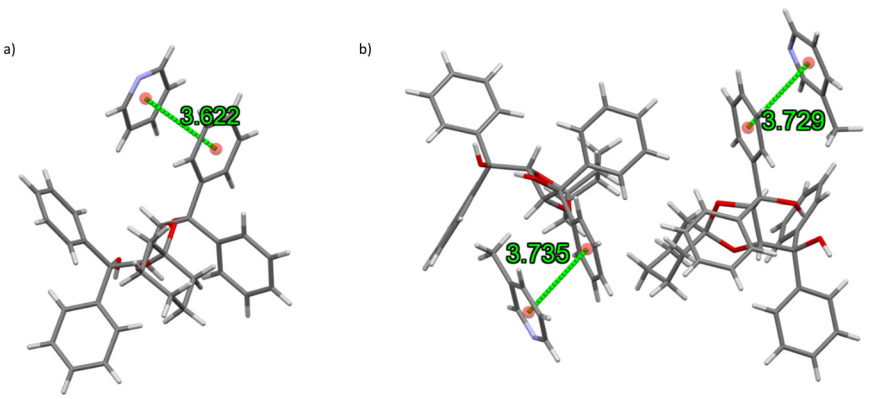

Fig. 5 The (host)π···π(guest) interactions (green lines, in Å) in the complexes of TADDOL6, which occurred only between the host and preferred ((a) PYR and (b) 3MP) guest species.

Table 3 Hydrogen bonding parameters in the pyridyl complexes with TADDOL6

Parameter	TADDOL6·PYR	TADDOL6·2MP	TADDOL6·3MP	TADDOL6·4MP
(Host)H···N(guest)/Å	1.91	1.88	1.87	1.91
		1.78[a]	1.88	1.91
		2.03[b]		
(Host)O···N(guest)/Å	2.713(3)	2.701(3)	2.660(3)	2.730(3)
		2.564(8)[a]	2.668(3)	2.749(3)
		2.791(4)[b]		
(Host)O–H···N(guest)/°	160	165	155	166
		155[a]	155	174
		151[b]		
Symmetry code	*x*, *y*, *z*	*x*, *y*, *z*	*x*, *y*, *z*	*x*, *y*, *z*
(Host)H···O(host)[c]/Å	1.85	1.83	1.82	1.86
		1.85	1.83	1.86
(Host)O···O(host)[c]/Å	2.688(2)	2.664(3)	2.663(2)	2.749(2)
		2.686(3)	2.667(2)	2.686(2)
(Host)O–H···O(host)[c]/°	173	176	177	169
		171	176	169

[a] 2MP disorder component 1. [b] 2MP disorder component 2. [c] These contacts are intramolecular in nature.

guests in the solution. At high concentrations of 3MP (60 and 80%), 3MP was favoured (though only extremely marginally in the former instance); 63.3 and 98.7% 3MP were measured in the mixed complexes, and the *K* values were 1.1 and 19.6, respectively. At high concentrations of PYR in the solution (60 and 80%), PYR was then the selected guest: these complexes contained 74.3 and 90.9% PYR; however, the *K* values were low in these two instances, 1.9 and 2.5. This investigation has demonstrated that TADDOL6 may be a suitable separatory host candidate for only the 20 : 80 PYR : 3MP mixture.

The data points contained in the plot provided in Fig. 2c (PYR/4MP) describe a host compound that is extremely selective, in this case in favour of PYR, when mixed with 4MP. Solutions containing 20, 40, 60 and 80% PYR afforded complexes with 95.7, 93.0, 97.8 and 100.0% of this guest, respectively. Consequently, the *K* values were extraordinary, 88.7, 19.8, 29.4 and infinite. All of these solutions may thus

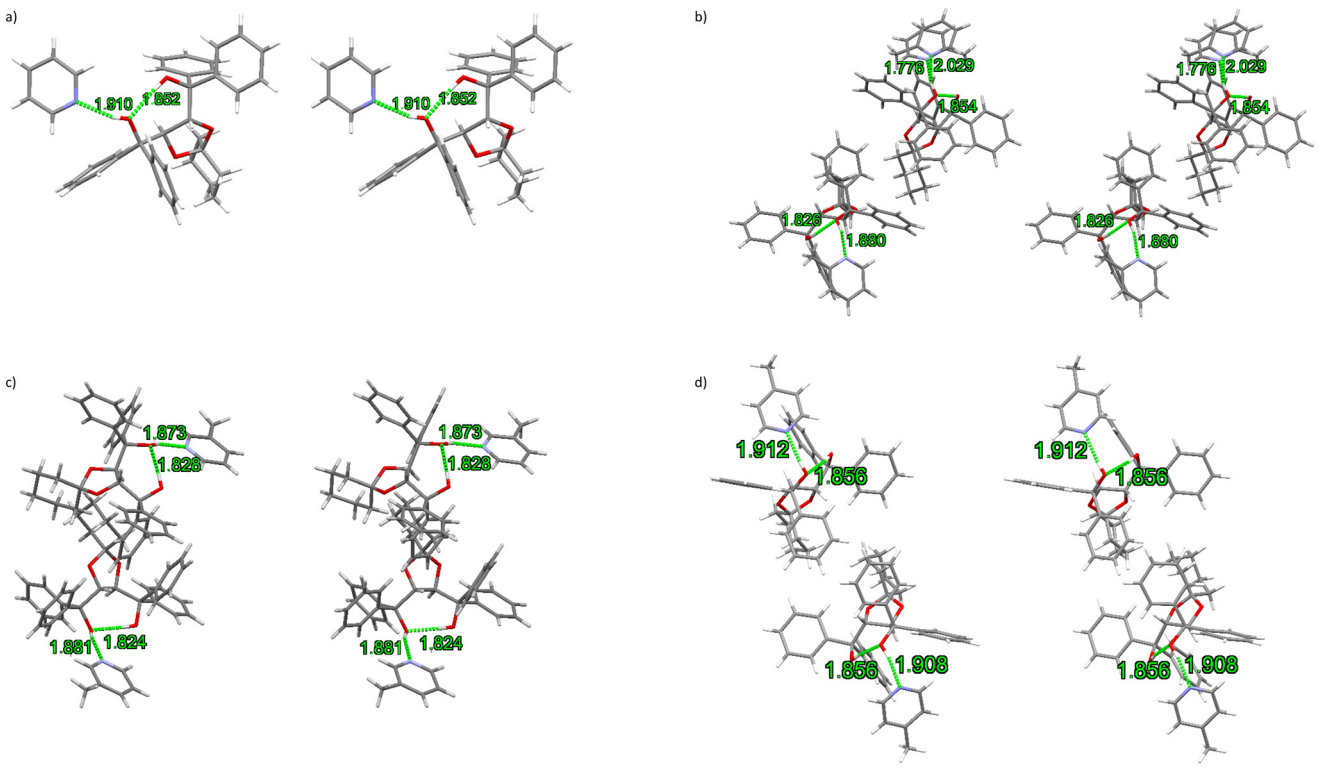

Fig. 6 Stereoscopic views of the hydrogen bonds in (a) TADDOL6·PYR, (b) TADDOL6·2MP, (c) TADDOL6·3MP and (d) TADDOL6·4MP.

be separated or purified by employing TADDOL6 as the host compound.

Once more, the plot in Fig. 2d (3MP/2MP) is S-shaped: a solution with only 20% 2MP provided a complex with 100.0% 3MP, while the 40, 60 and 80% 2MP solutions produced crystals in which only 2MP was detected (100.0%). In all four experiments, remarkably, K was infinite. These results are outstanding: TADDOL6 is therefore an excellent separatory host compound for these mixtures, selecting only 3MP when 20% 2MP was present, and only 2MP when 40, 60 or 80% 2MP were in the solution.

Fig. 2e (4MP/2MP) demonstrates, again, that the selectivity behaviour of TADDOL6 varied as the guest ratios changed. Only 4MP (100.0%) was observed in the crystals when the experiment employed a 20% 2MP solution. K was infinite. The 40% 2MP solution, on the other hand, produced crystals in which the host compound was, for all intents and purposes, unselective (the data point is very close to the line of no selectivity, where K = 1), while an increase in the amount of 2MP (60 and 80%) resulted in complexes with 72.1 and 100.0% of this guest. Here, the K values were 1.7 and infinite, respectively. Clearly, therefore, TADDOL6 may be employed to purify solutions with either 20% 2MP (in favour of 4MP) or 20% 4MP (in favour of 2MP).

From Fig. 2f (3MP/4MP), it is evident that TADDOL6 remained extremely selective for 3MP throughout. The 20, 40, 60 and 80% 3MP solutions afforded crystals with enhanced amounts of 3MP, 82.7%, 88.0%, 100.0% and 100.0%, respectively. From the first two of these, K values were significant, 19.1 and 11.1, while these values were infinite in the final two experiments. Therefore, all 3MP/4MP mixtures may be effectively separated by means of host–guest chemistry methodology with TADDOL6 as the host compound. These are notable results, given the near-identical boiling points of 3MP and 4MP (144 and 145 °C).

The only equimolar experiment result that did not adhere to the trends described in these plots for TADDOL6 was that of the 4MP/2MP mixture (Table 1). In that experiment, 98.7% 4MP was observed in the crystals, whilst this would be an extreme outlier when compared with the plot provided in Fig. 2e. It must be said though that, for TADDOL6, experiments in mixtures of these two guest solvents (2MP/4MP) were not straightforward, and many had to be repeated in order to obtain meaningful data points. Interestingly, these challenging experiments involved only the guests less preferred, thus explaining the ambivalent behaviour of the host compound.

3.4 Single crystal X-ray diffraction analyses on complexes of TADDOL6 with the pyridine guest solvents

The four pyridine complexes of TADDOL6 were subjected to SCXRD analyses, and the relevant crystallographic data for these are provided in Table 2. The complex with PYR, a favoured guest of this host compound, crystallized in the orthorhombic crystal system and space group $P2_12_12_1$, while the 2MP-containing inclusion compound with the least preferred guest species crystallized in the monoclinic crystal system and space group $P2_1$. Inclusion compounds with 3MP (preferred second to PYR) and 4MP (disfavoured), on the other hand, both crystallized in the triclinic crystal system (space group $P1$).

The only disorder observed was that in the complex with 2MP, this guest species experiencing rotational disorder. This observation may serve as one reason for the lower host affinity for 2MP since disorder alludes to a less dense crystal packing. Hirshfeld surface considerations agreed with this statement (see later).

A comparison of the unit cell dimensions and angles of the four complexes showed that the host packing was unique in each instance.

Fig. 3a–d depict the unit cell diagrams, while Fig. 4a–d illustrate the host–guest packing (left) and the void (right) diagrams for the four complexes.

Fig. 4a–d illustrate that the most preferred guest species of TADDOL6, PYR, experienced discrete cavity accommodation while the MP isomers were all housed in infinite channels.

The noncovalent host···host, host···guest and guest···guest interactions present in these complexes were subsequently investigated. The only host···guest π···π interactions observed in the pyridyl complexes were between TADDOL6 and the preferred PYR and 3MP guest molecules, one contact of this type in the former and two in the latter. Measurements were 3.622(1) Å (slippage 1.194 Å) for the complex containing PYR, and 3.735(1) and 3.729(1) Å (slippages 1.770 and 1.216 Å) for that with 3MP (Fig. 5a and b). There were no further π···π interactions in any of these complexes.

The host and guest molecules in each of the four complexes interacted through classical hydrogen bonding short contacts, facilitating the retention of the guest species in their crystalline complexes. Table 3 summarises the applicable parameters of these bonds. Moreover, the molecular geometry of TADDOL6 was also maintained by means of an intramolecular (host)O–H···O(host) classical hydrogen bonding interaction, the parameters of which are also contained in Table 3.

TADDOL6 possessed one unique hydrogen bond to PYR, two to 2MP (one to the ordered guest molecule, and one to each of the two disorder guest components; these 2MP molecules are crystallographically independent) and two unique bonds of this type to 4MP (also crystallographically independent). It was also noted that 3MP experienced two such interactions (both crystallographically independent). The applicable (host)H···N(guest), (host)O···N(guest) and (host)O–H···N(guest) parameters in the present investigation ranged between 1.78 and 1.91 Å, 2.564(8) and 2.791(4) Å, and 151 and 174° (Table 3). These are depicted in Fig. 6a–d, which are stereoscopic views for greater clarity. The parameters for

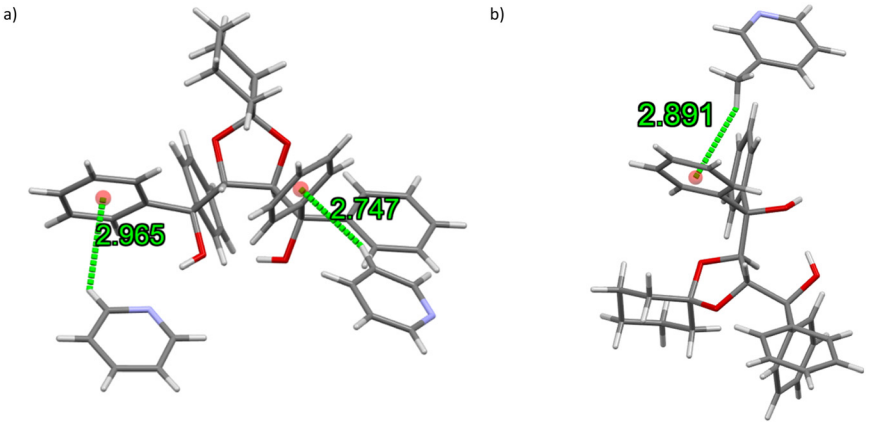

Fig. 7 The (guest)C–H···π(host) close contacts in (a) TADDOL6·PYR and (b) TADDOL6·3MP, containing the preferred guest species.

the intramolecular (host)O–H···O(host) contacts were 1.82–1.86 Å, 2.663(2)–2.688(2) Å, and 169–177°.

In a previous report, the hydrogen bond distances (and angles) were effectively used to explain the selectivity order for these guest compounds when employing an alternative TADDOL-derived host compound,[42] but in the present case, these distances were comparably long in the complexes with PYR (the preferred guest compound) and 4MP (disfavoured), while both 2MP (not preferred) and 3MP (a favoured guest species) experienced, generally, similar short contacts of this type with TADDOL6 (Table 3). Therefore, a consideration of such bond parameters here does not support the observed host selectivity order for these pyridines.

Additionally, in each of the four complexes was identified C–H···π short contacts between the host and guest molecules. In TADDOL6·PYR (containing a preferred guest species, Fig. 7a), two interactions of this type were observed, involving the *ortho* and *meta* hydrogen atoms of the guest species and the centre of gravity (Cg) of a host aromatic moiety, which measured 2.97 and 2.75 Å (H···Cg), 3.648(3) and 3.639(3) Å (C···Cg), and 130 and 157° (C–H···Cg). Only one such interaction was observed in the TADDOL6·3MP complex (also a favoured guest, Fig. 7b), involving one of the guest hydrogen atoms of the *meta*-methyl substituent and the phenyl ring of the host species; measurements were 2.89 Å, 3.645(3) Å, and 144°.

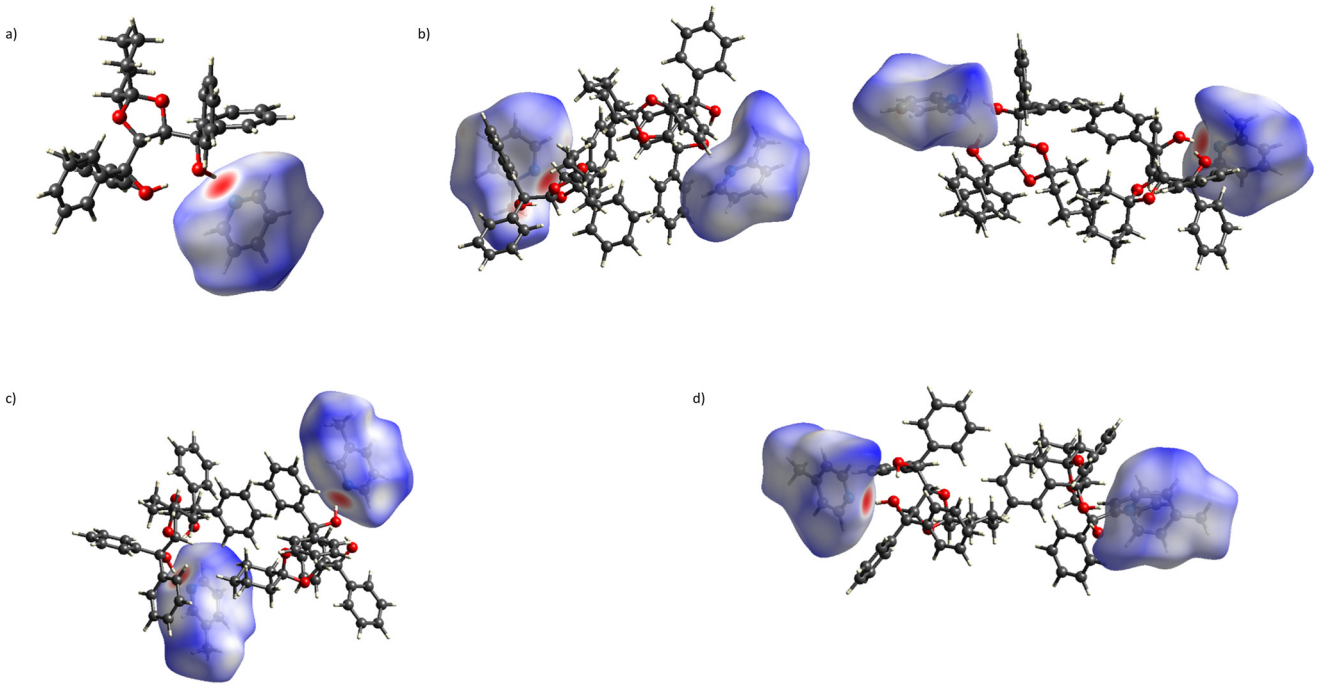

Fig. 8 Three-dimensional Hirshfeld surfaces around the guest molecules in (a) TADDOL6·PYR, (b) TADDOL6·2MP (combined ordered and disorder guest component 1, left), TADDOL6·2MP (combined ordered and disorder guest component 2, right), (c) TADDOL6·3MP (combined for both guest molecules) and (d) TADDOL6·4MP (combined for both guest molecules); the red areas represent strong (guest)N···H–O(host) hydrogen bonding interactions.

These kinds of interactions were also present in the complexes with guests less preferred (2MP and 4MP) and were (guest)C–H···π(guest), (host)C–H···π(guest) and (guest) C–H···π(host) in nature, with applicable measurements ranging between 2.67 and 2.99 Å, 3.543(4) and 3.787(3) Å, and 153 and 139°.

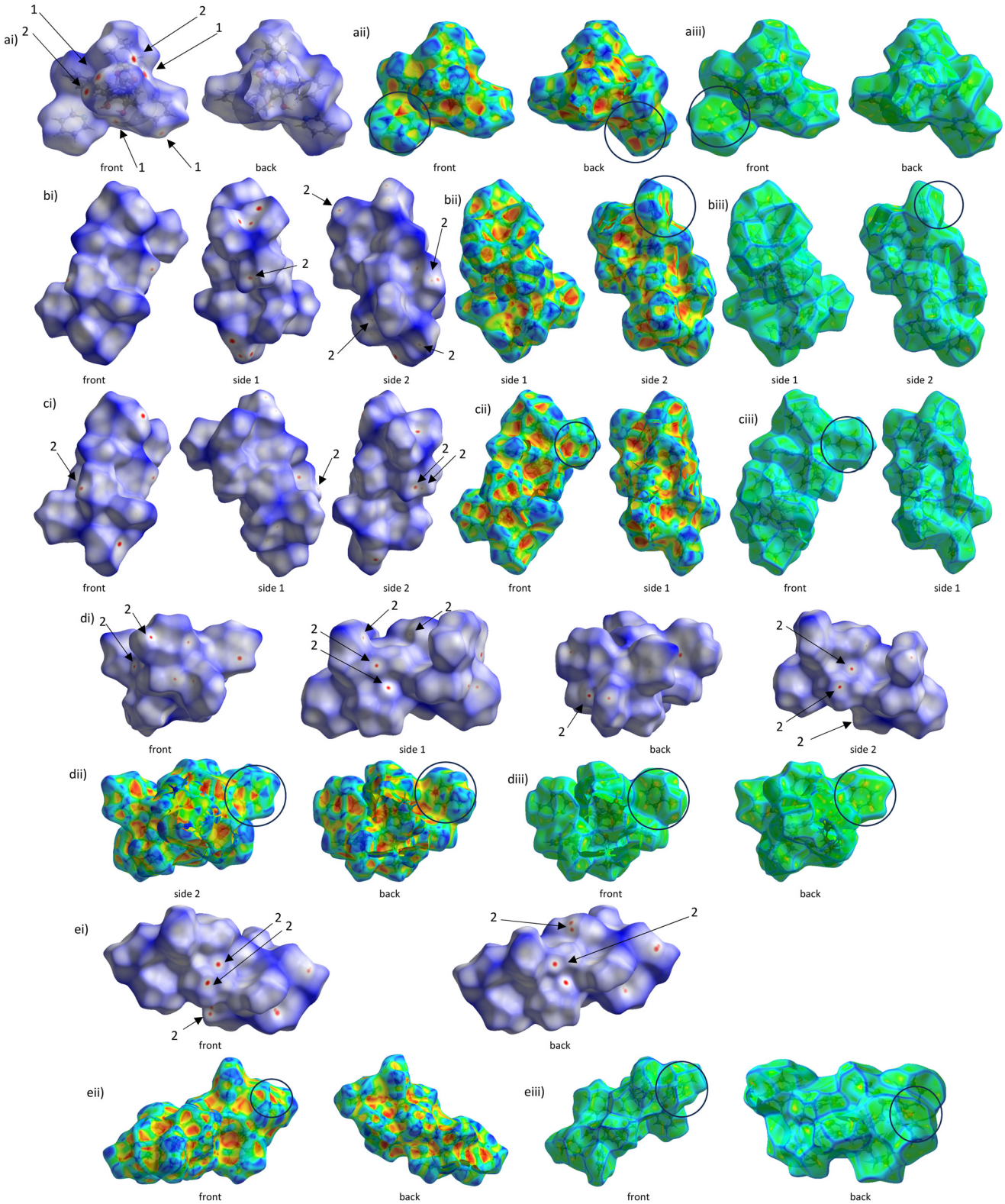

Fig. 9 Surfaces for d_{norm} (labelled as i), shape index (ii) and curvedness (iii) for the complexes (a) TADDOL6·PYR, (b) TADDOL6·2MP (disorder guest component 1), (c) TADDOL6·2MP (disorder guest component 2) (d) TADDOL6·3MP and (e) TADDOL6·4MP.

3.5 Hirshfeld surfaces and the two-dimensional fingerprint plots

Fig. 8a–d illustrate the Hirshfeld surfaces that were generated around the guest molecules of the complexes with TADDOL6. The red areas represent the hydrogen bonding close contacts between the host and guest species.

In Fig. 9, the d_{norm} surfaces (labelled ai, bi, *etc.*) are composed of blue, red and white areas. The red areas indicate shorter contacts with a negative potential with electrophilic characteristics, the blue areas show longer contacts with a positive potential with nucleophilic characteristics, and the white areas approximate the van der Waals radii.[43,44] The red dots labelled 1 in Fig. 9ai indicate the O–H···O bonding, while the red dots labelled 2 (Fig. 9ai–ei) represent the H···H interactions. In Fig. 9a, it is clear that both hydrogen bonding and H···H contacts are present, while in Fig. 9bi–ei are observed only H···H interactions. The H-bonding between host and guest do not feature on the surfaces in these latter three figures since the guest molecules occupied endless channels within the crystal structures and host···guest hydrogen bonding was within these channels, while in the PYR-containing complex (Fig. 9ai), the guest being housed in discrete cavities, the H-bonds are then visible on this surface. Other red dots not labelled signify other contact types, including C···C and π···π stacking interactions.

The shape index (Fig. 9aii–eii) and curvedness (Fig. 9aiii–eiii) analyses further highlight the π···π stacking interactions in the four complexes. In the former, the adjacent concave (red triangles) and convex (blue triangles) areas allude to such π···π stacking interactions, these being encircled in black. The Hirshfeld surfaces mapped with curvedness possess some flat areas, also encircled in black, which show the ring contributions to these interactions.

Fig. 10 is a bar graph that summarises the quantities (%) of the various interactions between the host and guest species, while Fig. 11a–d illustrate the Hirshfeld 2D fingerprint plots that were obtained from the 3D plots presented in Fig. 8a–d. Interestingly, these 2D plots, which

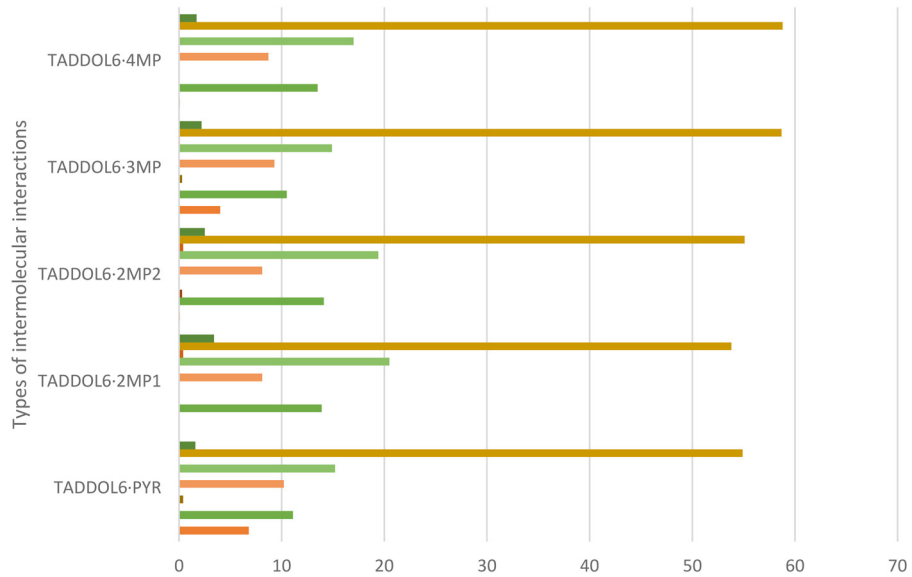

	TADDOL6·PYR	TADDOL6·2MP1	TADDOL6·2MP2	TADDOL6·3MP	TADDOL6·4MP
H···O	1.6	3.4	2.5	2.2	1.7
H···H	54.9	53.8	55.1	58.7	58.8
H···N	0	0.4	0.4	0.1	0
H···C	15.2	20.5	19.4	14.9	17
N···O	0	0	0	0	0
N···H	10.2	8.1	8.1	9.3	8.7
N···N	0	0	0	0	0
N···C	0.4	0	0	0.3	0
C···O	0	0	0.3	0	0
C···H	11.1	13.9	14.1	10.5	13.5
C···N	0	0	0	0	0
C···C	6.8	0	0.1	4	0.1

Fig. 10 Types and contributions of the intermolecular guest···host interactions in TADDOL6·PYR, TADDOL6·2MP1 (disorder guest component 1), TADDOL6·2MP2 (disorder guest component 2), TADDOL6·3MP and TADDOL6·4MP.

reflect the distances between the nearest host atom on the outside of the surface (d_e) and guest atom on its inside (d_i) clearly demonstrate that the crystal packing in the PYR- and 3MP-containing complexes is significantly tighter than in the complexes with disfavoured 2MP and 4MP as is observed by the shorter d_e and d_i ranges in the former two inclusion compounds, furnishing yet another reason for the host affinity for PYR and 3MP. In fact, this plot for unpreferred 2MP is the most diffuse of all, and possibly explains why the selectivity of TADDOL6 for 2MP was so low (the complex experienced a relatively loose crystal packing).

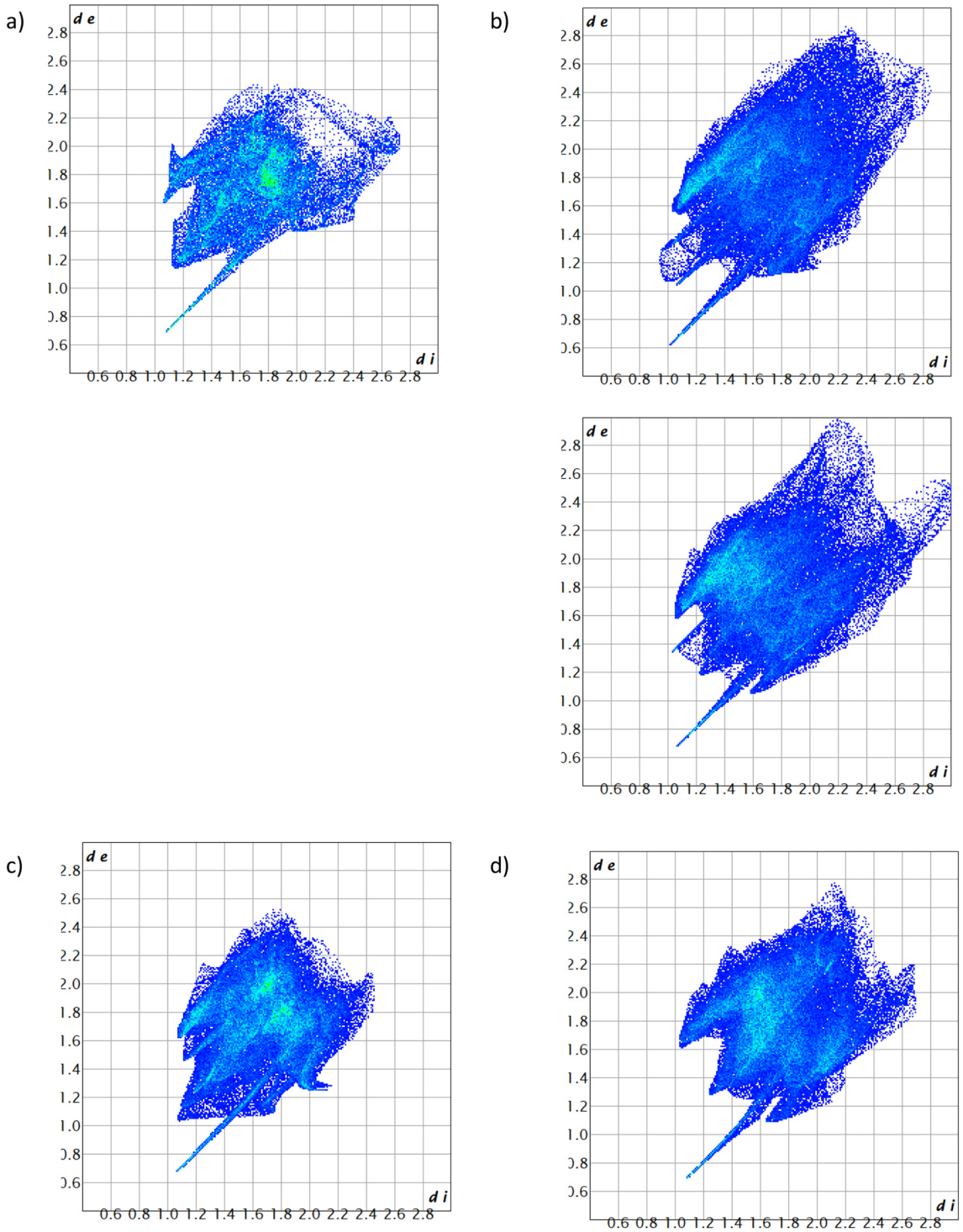

Fig. 11 Hirshfeld fingerprint plots illustrating all G···H interactions in (a) TADDOL6·PYR, (b) TADDOL6·2MP (combined ordered guest and disorder guest component 1, top), TADDOL6·2MP (combined ordered guest and disorder guest component 2, bottom), (c) TADDOL6·3MP (combined for both guest molecules) and (d) TADDOL6·4MP (combined for both guest molecules).

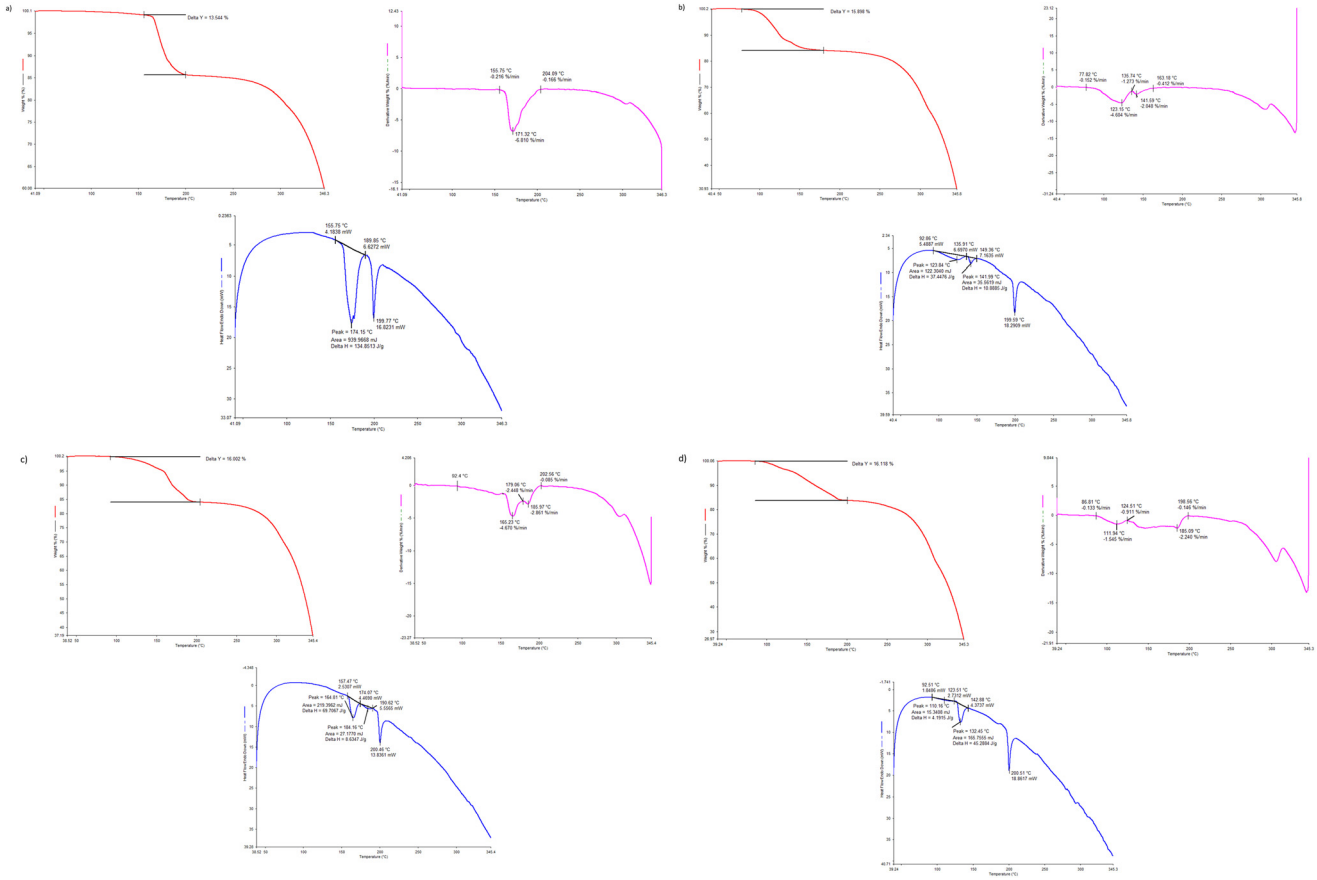

Fig. 12 The DSC (blue, endo down), TG (red) and DTG (magenta) traces for each of (a) TADDOL6·PYR, (b) TADDOL6·2MP, (c) TADDOL6·3MP and (d) TADDOL6·4MP.

3.6 Thermal analyses

The four complexes of TADDOL6 were subjected to thermal analyses, and the overlaid differential scanning calorimetry (DSC), thermogravimetry (TG) and its derivative (DTG) traces are provided in Fig. 12a–d, while Table 4 is a summary of the more applicable data from these plots.

The theoretical mass losses required for the guest release processes upon heating these 1:1 H:G complexes with TADDOL6 agreed closely with those expected: the complexes with PYR, 2MP, 3MP and 4MP experienced mass losses of 13.5, 15.9, 16.0 and 16.1%, while the calculated values were 13.5 (PYR) and 15.5% (the MP isomers) (Table 4).

Each of the complexes was characterised by two guest release events (whether these be broad or sharp, dependent on the guest), followed by an endotherm (around 200 °C, the peak temperature) representing the host melt.

When one considers the relative thermal stabilities of these complexes by measuring the guest release onset temperatures (T_{on}, estimated from the DTGs), it may be concluded that this stability decreased in the order TADDOL6·PYR (155.8 °C) > TADDOL6·3MP (92.4 °C) > TADDOL6·4MP (86.8 °C) > TADDOL6·2MP (77.8 °C) (Table 4). Once more, this is in direct accordance with the host selectivity observations that were made in the guest competition experiments as well as with the results obtained from the Hirshfeld surface analyses: the stabilities of these complexes increased with an increasing host affinity for the pyridyl guest compound.

Finally, the enthalpies of the guest release event in each case, which describes the amount of energy required in order to break the noncovalent bonds between host and guest species in these complexes, also agreed with the selectivity

Table 4 Relevant thermoanalytical data for the complexes of TADDOL6 with the pyridine guest solvents[a]

Complex	T_{on}/°C	Enthalpy (ΔH)/J g^{-1}	Mass loss expected/%	Mass loss measured/%
TADDOL6·PYR	155.8	134.9	13.5	13.5
TADDOL6·2MP	77.8	48.3	15.5	15.9
TADDOL6·3MP	92.4	78.3	15.5	16.0
TADDOL6·4MP	86.8	49.5	15.5	16.1

[a] T_{on}, a measure of the thermal stability of the complexes, is the guest release onset temperature.

behaviour of TADDOL6. The enthalpy for the complex with preferred PYR was significantly greater (134.9 J g^{-1}) than for the remaining complexes and, additionally, that for TADDOL6·3MP (also having a favoured guest solvent) was greater (78.3 J g^{-1}) relative to those complexes with guests not preferred (2MP and 4MP, 48.3 and 49.5 J g^{-1}, respectively).

Conclusions

TADDOL6 formed 1 : 1 H : G inclusion compounds with each of PYR, 2MP, 3MP and 4MP when crystallized from these organic solvents. From crystallization experiments of TADDOL6 from guest mixtures, it was demonstrated that the host selectivity for these guests was in the order PYR > 3MP > 4MP > 2MP. It was further shown that TADDOL6 has the ability to separate very many of the pyridine mixtures considered in this work owing to extremely high host selectivities. SCXRD experiments revealed that only the favoured guest species, PYR and 3MP, were involved in (host)π···π(guest) stacking interactions (3.622(1) Å for the PYR-containing complex, and 3.735(1) and 3.729(1) Å for the two crystallographically independent 3MP guest molecules in TADDOL6·3MP). Furthermore, each of the guest species in the four complexes were retained in the crystals of their complexes by means of classical (host)O–H···N(guest) hydrogen bonds, while an intramolecular (host)O–H···O(host) interaction maintained the host molecular geometry in each instance. Gratifyingly, observations in both Hirshfeld surface and thermal (when noting T_{on} and the enthalpy associated with the guest release events) analyses were in direct accordance with the selectivity order of the host compound for these guest solvents: preferred guests PYR and 3MP formed the more stable complexes, possessed a tighter packing and had higher enthalpies (for the guest release event) compared with those containing 2MP and 4MP.

Data availability

The crystal structures of complexes TADDOL6·PYR, TADDOL6·2MP, TADDOL6·3MP and TADDOL6·4MP were deposited at the Cambridge Crystallographic Data Centre (CCDC) and their CCDC numbers are 2341183, 2341184, 2341185 and 2341186.

Author contributions

D. L. R.: investigation; methodology; validation; writing the original draft. B. B.: conceptualization; funding acquisition; methodology; project administration; resources; supervision; visualization; assistance with editing the original draft. E. C. H.: data curation; formal analysis.

Conflicts of interest

There are no conflicts of interest to declare.

Acknowledgements

Financial support is acknowledged from the Nelson Mandela University and the National Research Foundation (South Africa).

References

1 Y. Zeng, C. Liang, X. Lu, L. Zhao, F. Wu, T. Hou, A. Zhao, M. Lv, Z. Tao and Q. Li, Perfect separation of pyridine and 3-methylpyridine by cucurbit[6]uril, *Chin. Chem. Lett.*, 2024, 110807.
2 N. M. Cullinane, S. J. Chard and R. Meatyard, The preparation of methylpyridines by catalytic methods, *J. Soc. Chem. Ind.*, 1948, **67**, 142–143.
3 I. Y. Lazdin'sh and A. A. Avot-s, Separation of pyridine compounds on ion-exchange resins, *Chem. Heterocycl. Compd.*, 1971, **7**, 202–206.
4 Y. Shen, J. Zhu, C. Wang and H. Qiu, Process of separating methyl pyridine mixture, CN101066946A, 2007.
5 E. Coulson and J. Jones, Studies in coal tar bases. I. Separation of β- and γ-picolines and 2:6-lutidine, *J. Soc. Chem. Ind.*, 1946, **65**, 169–175.
6 N. G. Grigor'eva, N. A. Filippova, M. I. Tselyutina and B. I. Kutepov, Synthesis of pyridine and methylpyridines over zeolite catalysts, *Appl. Petrochem. Res.*, 2015, **5**, 99–104.
7 E. F. V. Scriven and R. Murugan, Pyridine and pyridine derivatives, *Kirk-Othmer Encyclopedia of Chemical Technology*, John Wiley & Sons, Ltd, 2005.
8 R. V. Hoffman, *Organic chemistry: An intermediate text*, John Wiley & Sons, Inc., 2004.
9 A. E. Chichibabin and M. P. Oparina, Über die synthese des pyridins aus aldehyden und ammoniak, *J. Prakt. Chem.*, 1924, **107**, 154–158.
10 A. P. Ivanovskii, V. A. Shikanov, K. M. Kut'in and M. A. Korshunov, Synthesis of pyridine and β-picoline from acetaldehyde, formaldehyde, and ammonia, *Khim. Prom-st.*, 1972, **48**, 26–28.
11 R. Bicker, H. Deger, W. Herzog, K. Rieser, H. Pulm, G. Hohlneicher and H.-J. Freund, X-ray photoelectron spectroscopy study of silica-alumina catalysts used for a new pyridine synthesis, *J. Catal.*, 1985, **94**, 69–78.
12 M. Yoshizo, Process for producing pyridine bases, US3946020, 1976.
13 J. J. Mao, D. Y. Weimini and L. Guanzhong, Influence of loading of Co/Pb-ZSM-5 zeolite catalysts on yield of pyridine bases, *Huagong Shikan*, 2003, **17**, 24–27.
14 F. J. van Der Gaag, F. Louter, J. C. Oudejans and H. van Bekkum, Reaction of ethanol and ammonia to pyridines over zeolite ZSM-5, *Appl. Catal.*, 1986, **26**, 191–201.
15 S. Shimizu, N. Abe, A. Iguchi, M. Dohba, H. Sato and K. I. Hirose, Synthesis of pyridine bases on zeolite catalyst, *Microporous Mesoporous Mater.*, 1998, **21**, 447–451.
16 K. Suresh Kumar Reddy, I. Sreedhar and K. V. Raghavan, Interrelationship of process parameters in vapor phase pyridine synthesis, *Appl. Catal., A*, 2008, **339**, 15–20.

17 K. Suresh Kumar Reddy, I. Sreedhar and K. V. Raghavan, Kinetic studies on vapour phase pyridine synthesis and catalyst regeneration studies, *Can. J. Chem. Eng.*, 2011, **89**, 854–863.
18 H. Sato, S. Shimizu, N. Abe and K. Hirose, Synthesis of pyridine bases over ion-exchanged pentasil zeolite, *Chem. Lett.*, 1994, **23**, 59–62.
19 W. M. Haynes, *CRC Handbook of Chemistry and Physics*, 98th edn, 2016.
20 K. Suresh Kumar Reddy, C. Srinivasakannan and K. V. Raghavan, Catalytic vapor phase pyridine synthesis: A process review, *Catal. Surv. Asia*, 2012, **16**, 28–35.
21 J. W. Steed and J. L. Atwood, *Supramolecular Chemistry*, John Wiley & Sons, Ltd, United States of America, 2022.
22 J.-M. Lehn, Supramolecular Chemistry, *Proc. - Indian Acad. Sci., Chem. Sci.*, 1994, **106**, 915–922.
23 J. Bacsa, M. R. Caira, A. Jacobs, L. R. Nassimbeni and F. Toda, Complexation with diol host compounds. Part 33. Inclusion and separation of pyridines by a diol host compound, *Cryst. Eng.*, 2000, **3**, 251–261.
24 S. A. Bourne, K. C. Corin, L. R. Nassimbeni and F. Toda, Selective enclathration of picolines, *Cryst. Growth Des.*, 2005, **5**, 379–382.
25 B. Barton, E. C. Hosten and D. V. Jooste, Comparative investigation of the inclusion preferences of optically pure versus racemic TADDOL hosts for pyridine and isomeric methylpyridine guests, *Tetrahedron*, 2017, **73**, 2662–2673.
26 B. Barton, M. R. Caira, D. V. Jooste and E. C. Hosten, Investigation of the separation potential of xanthenyl- and thioxanthenyl-based host compounds for pyridine and isomeric picoline mixtures, *J. Inclusion Phenom. Macrocyclic Chem.*, 2020, **98**, 223–235.
27 B. Barton, M. R. Caira, D. B. Trollip and E. C. Hosten, The behaviour of tricyclic fused host systems comprising seven-membered B-rings in mixed pyridines, *CrystEngComm*, 2023, **25**, 6317–6328.
28 B. Barton, M. R. Caira, U. Senekal and E. C. Hosten, Selectivity considerations of host compound trans-9,10-dihydro-9,10-ethanoanthracene-11,12-dicarboxylic acid when presented with pyridine and picoline mixtures: Charge-assisted versus classical hydrogen bonding, *CrystEngComm*, 2022, **24**, 4573–4583.
29 B. Barton, J. Vorgers and E. C. Hosten, The behaviour of the wheel-and-axle host compound 1,4-bis(diphenylhydroxymethyl) benzene in mixed pyridyl guest solvents, *Cryst. Growth Des.*, 2023, **23**, 6641–6650.
30 A. Bruker, *APEX2, SADABS and SAINT*, Bruker AXS Inc., Madison (WI), USA, 2010.
31 G. M. Sheldrick, SHELXT – Integrated space-group and crystal structure determination, *Acta Crystallogr., Sect. A: Found. Adv.*, 2015, **71**, 3–8.
32 G. M. Sheldrick, Crystal structure refinement with SHELXL, *Acta Crystallogr., Sect. C: Struct. Chem.*, 2015, **71**, 3–8.
33 C. B. Hübschle, G. M. Sheldrick and B. Dittrich, ShelXle: A Qt graphical user interface for SHELXL, *J. Appl. Crystallogr.*, 2011, **44**, 1281–1284.
34 Bruker, *APEX4, SAINT, SADABS*, Bruker AXS Inc., Madison, Wisconsin, USA, 2012.
35 L. J. Farrugia, WinGX and ORTEP for Windows: An update, *J. Appl. Crystallogr.*, 2012, **45**, 849–854.
36 G. M. Sheldrick, Crystal structure refinement with SHELXL, *Acta Crystallogr., Sect. C: Struct. Chem.*, 2015, **71**, 3–8.
37 B. Barton, The synthesis of clathrate hosts for enantiomer separation, *MSc Dissertation*, University of Port Elizabeth, Port Elizabeth, South Africa, 1993.
38 A. M. Pivovar, K. T. Holman and M. D. Ward, Shape-selective separation of molecular isomers with tunable hydrogen-bonded host frameworks, *Chem. Mater.*, 2001, **13**, 3018–3031.
39 C. F. Macrae, I. Sovago, S. J. Cottrell, P. T. A. Galek, P. McCabe, E. Pidcock, M. Platings, G. P. Shields, J. S. Stevens, M. Towler and P. A. Wood, Mercury 4.0: From visualization to analysis. Design and prediction, *J. Appl. Crystallogr.*, 2020, **53**, 226–235.
40 M. A. Spackman and D. Jayatilaka, Hirshfeld surface analysis, *CrystEngComm*, 2009, **11**, 19–32.
41 P. R. Spackman, M. J. Turner, J. J. McKinnon, S. K. Wolff, D. J. Grimwood, D. Jayatilaka and M. A. Spackman, CrystalExplorer: A program for Hirshfeld surface analysis, visualization and quantitative analysis of molecular crystals, *J. Appl. Crystallogr.*, 2021, **54**, 1006–1011.
42 D. L. Recchia, B. Barton and E. C. Hosten, Exploring supramolecular chemistry as an innovative strategy for pyridine guest separations when employing a TADDOL derivative as the host compound, *Cryst. Growth Des.*, 2024, **24**, 6438–6449.
43 R. D. Nagdeve, J. S. Thakur, S. Chandrashekharappa, K. M. Bairagi, P. K. Deb, K. N. Venugopala, P. K. Mondal, M. Polentarutti, O. I. Alwassil, V. Mohanlall and S. K. Nayak, Crystal structure, hydrogen bonding interactions, Hirshfeld surfaces, energy frameworks, and DFT calculation of Diethyl 3-(4-substitutedbenzoyl)indolizine-1,2-dicarboxylates, *J. Mol. Struct.*, 2024, 138080, DOI: **10.1016/j.molstruc.2024.138080**.
44 R. D. Nagdeve, J. S. Thakur, S. Chandrashekharappa, P. K. Mondal, P. K. Deb, M. Polentarutti, K. M. Bairagi, G. Rakshit, O. I. Alwassil, M. Pillay, K. N. Venugopala and S. K. Nayak, Structural analysis, in vitro anti-tubercular activities, and in silico ADMET evaluation of ethyl 7-methoxy-3-(4-substituted benzoyl)indolizine-1-carboxylates, *CrystEngComm*, 2025, DOI: **10.1039/D4CE01018C**.

